JOURNAL OF GEOPHYSICAL RESEARCH, VOL. 99, NO. D11, PAGES 23,131-23,148, NOVEMBER 20, 1994

NCAR CCM2 simulation of the modern Antarctic climate

Ren-Yow Tzeng,[1] David H. Bromwich,[2,3] Thomas R. Parish,[4] and Biao Chen[2]

Abstract. The National Center for Atmospheric Research community climate model version 2 (CCM2) simulation of the circumpolar trough, surface air temperature, the polar vortex, cloudiness, winds, and atmospheric moisture and energy budgets are examined to validate the model's representation of the present-day Antarctic climate. The results show that the CCM2 can well simulate many important climate features over Antarctica, such as the location and intensity of the circumpolar trough, the coreless winter over the plateau, the intensity and horizontal distribution of the surface inversion, the speed and streamline pattern of the katabatic winds, the double jet stream feature over the southern Indian and Pacific oceans, and the arid climate over the continent. However, there are also some serious errors in the model. Some are due to old problems but some are caused by the new parameterizations in the model. The model errors over high southern latitudes can be summarized as follows: The circumpolar trough, the polar vortex, and the westerlies in midlatitudes are too strong; the semiannual cycle of the circumpolar trough is distorted compared to the observations; the low centers of the circumpolar trough and the troughs in the middle and upper troposphere are shifted eastward by 15°-40° longitude; the surface temperatures are too cold over the plateau in summer and over the coastline in winter; the polar tropopause continues to have a cold bias; and the cloudiness is too high over the continent. These biases are induced by two major factors: (1) the cloud optical properties in tropical and middle latitudes, which cause the eastward shift of troughs and surface low centers and the error in the semiannual cycle, and (2) the cold bias of the surface air temperature, which is attributed to the oversimulation of cloudiness over the continent, especially during summer, and the uniform 2-m-thick sea ice. The constant thickness of sea ice suppresses the energy flux from the ocean to the atmosphere and hence reduces the air temperature near the coast during winter. Finally, although the simulated Antarctic climate still suffers these biases, the overall performance of the CCM2 is much better than that of the CCM1-T42. Therefore the CCM2 is good enough to be used for climate change studies, especially over Antarctica.

1. Introduction

The atmosphere over Antarctica and the surrounding ocean constitutes not only one of the largest energy sinks on Earth but also plays an important role in controlling the variability of global climate. Recently, many general circulation models (GCMs) have simulated the maximum surface temperature increase over these regions in response to doubled atmospheric CO_2 concentrations [*Intergovernmental Panel on Climate Control (IPCC)*, 1990]. *Meehl* [1987] and *Meehl and Albrecht* [1988] indicated that the behavior of the circumpolar trough in high southern latitudes is associated with anomalies of tropical sea surface temperatures. Furthermore, *Bromwich et al.* [1993] pointed out that blocking over East Antarctica is associated with an intensification of the southern branch of the split jet stream over the New Zealand sector as well as enhanced storm activity in that region and in other areas of the southern hemisphere.

However, many atmospheric GCMs fail to adequately simulate some important climatological features over high southern latitudes, such as the circumpolar trough, the

[1]Department of Atmospheric Sciences, National Central University, Chungli, Taiwan.
[2]Polar Meteorology Group, Byrd Polar Research Center, Ohio State University, Columbus.
[3]Also at Atmospheric Sciences Program, Ohio State University, Columbus.
[4]Department of Atmospheric Science, University of Wyoming, Laramie.

Paper number 94JD02156.
0148-0227/94/94JD-02156$05.00

double jet stream over the New Zealand area, and the semiannual variation of winds and sea level pressures [e.g., *Xu et al.*, 1990]. The previous version of the National Center for Atmospheric Research (NCAR) community climate model (CCM) (version 1, CCM1) also has some of these deficiencies [*Tzeng et al.*, 1993]; e.g., the location of circumpolar trough is not properly simulated due to insufficient horizontal resolution, and the polar front part of the split jet stream over the New Zealand sector in winter is too weak due to a bias in the simulated thermal forcing. In addition, the CCM1 simulates too much precipitation over Antarctica due to an artificial positive moisture fixer scheme. By contrast, the new generation of the NCAR CCM, the CCM2, uses a semi-Lagrangian method to transport moisture and other trace constituents instead of the spectral method with the positive moisture fixer scheme [*Williamson and Rasch,* 1994]. This transport scheme has been shown to produce much better simulations of local atmospheric moisture budgets, such as over the North Polar Cap [*Bromwich et al.*, 1994]. Moreover, many of the above-mentioned biases in CCM1 are expected to be improved by CCM2. Here, we examine this question for high southern latitudes.

Some other aspects regarding CCM2 performance are also documented by other researchers [e.g., *Hack et al.*, 1994; *Kiehl et al.*, 1994]. Kiehl et al. indicated that the model simulates too much incoming shortwave radiation and emits too much longwave radiation primarily because of deficiencies in the cloud optical properties. However, these studies emphasize the tropics and midlatitudes. Therefore this paper concentrates on the model simulations over high southern latitudes.

2. The Model and Data

The major modifications to the model architecture from CCM1 to CCM2 are described in detail by *Hack et al.* [1993] and *Hurrel et al.* [1993]. The standard version of the NCAR CCM2 is at T42 (triangular truncation at wavenumber 42) horizontal resolution (about 2.8° latitude x 2.8° longitude) with 18 vertical levels in a hybrid coordinate system (0.993, 0.970, 0.929, 0.866, 0.787, 0.695, 0.598, 0.501, 0.409, 0.325, 0.251, 0.189, 0.139, 0.099, 0.064, 0.032, 0.013, 0.005), while the CCM1 is at R15 horizontal resolution with 12 pure vertical sigma levels.

The numerical schemes and physical parameterizations of the CCM2 are described in detail by *Hack et al.* [1993]. The principal algorithmic approaches that have been carried forward from CCM1 to CCM2 are a semi-implicit/leap-frog time integration scheme, the spectral transform method for treating dry dynamics, a biharmonic horizontal-diffusion operator, and the formulation of the stable condensation process. The CCM2 includes a semi-Lagrangian scheme for transporting water vapor, cloud water, and chemical constituents [*Williamson and Rasch,* 1994]. This scheme is used to improve the transport of all positive-definite quantities in the spectral model, which creates negative values due to spectral truncation. A comparison between this scheme and the positive moisture fixer scheme used in the CCM1 is presented by *Rasch and Williamson* [1990]. Unlike the physical parameterizations in CCM1, in which convection and surface hydrology are based on Geophysical Fluid Dynamics Laboratory physics [*Manabe et al.*, 1965] and the treatment of clouds and radiation follows *Ramanathan et al.* [1983], the physical parameterizations in CCM2 are almost completely new. The radiation calculation includes molecular, cloud, and surface scattering, along with H_2O, O_3, CO_2, O_2, cloud, and surface absorption. The cloud emissivity depends on liquid water path [*Kiehl et al.*, 1994]. The model incorporates a Voigt correction to the longwave cooling in the upper stratosphere and a new cloud albedo and fraction parameterization [*Slingo,* 1987]. A stability-dependent mass-flux scheme is used to represent all types of moist convective processes [*Hack,* 1994]. The model includes an explicit prediction of the planetary boundary layer height and turbulence velocity scale, which is also important for the formation of low clouds over the Arctic basin [*Randall et al.*, 1985].

The sea surface temperature (SST) and sea-ice distributions are specified by climatological data and updated in the middle of each month for seasonal cycle simulations. However, the SST data used in CCM2 are from *Shea et al.* [1990] that differ from those in CCM1 [*Alexander and Mobly,* 1976]. The seasonal cycle of the model is basically forced by the seasonal change of SST and the daily change of the solar declination angle with a fixed solar insolation (1370 W m^{-2}) at the top of the model atmosphere. The diurnal cycle of insolation is also included in the CCM2, but it is absent from the CCM1. The diurnal cycle may affect the calculation of surface temperature and the stability of the surface layer during nighttime [*Hansen et al.*, 1983], but this effect is small in the polar regions [e.g., *Herman and Goody,* 1976].

The control run of this version of CCM2 was integrated for 20 model years by NCAR (CCM2 case number 388). This paper, however, analyzes only 5 years (years 11-15) of model output to maintain consistency with the analysis of CCM1 [*Tzeng et al.*, 1993]. For the purpose of this paper, the results from 5-model year averages represent the climatology of 20-model years, as judged from the comparison of 5-year means with 20-year means for several model variables. The model results are validated against the European Center for Medium-Range Weather Forecasts/World Meteorological Organization (ECMWF/WMO) archived observational data set from NCAR.

This archive is available at seven levels from 1000 to 100 hPa, has a resolution of 2.5° latitude x 2.5° longitude, and spans 1980 to 1989 at intervals of 12 hours.

3. Results

3.1. Circumpolar Trough

The circumpolar trough is one of the important climate features over high southern latitudes. It links the katabatic wind regime over Antarctica with the large-scale tropospheric circulation in middle latitudes [*Parish et al.*, 1994; *Egger*, 1992]. Most GCMs can reflect its existence but cannot capture its location and intensity correctly. *Hart et al.* [1990] and *Boville* [1991] found that the simulated circumpolar trough in sea level pressure is significantly improved by increasing the horizontal resolution of their GCMs, BMRC and CCM1, respectively. Furthermore, *Tzeng et al.* [1993] indicated that the errors in the latitudinal location and the intensity (too weak) of the circumpolar trough simulated by CCM1-R15 are mainly due to the distortion of the topography by the low horizontal resolution. By increasing the horizontal resolution, CCM2-T42 can well simulate the latitudinal location of the circumpolar trough. However, the low centers are shifted eastward by 15°-40° longitude, and the intensity is too strong (Figure 1). The eastward shift of these low centers is consistent with the eastward shift of the planetary-scale waves in the middle and upper troposphere, discussed below. In addition, the oversimulation of the low centers partly results from the surface temperature cold bias, as discussed in section 3.3 on 500-hPa height.

On the other hand, *Meehl* [1987] and *Meehl and Albrecht* [1988] found that the change of the intensity of the circumpolar trough is related to the SST anomalies and hence the intensity of tropical heating. This connection suggests that the errors in the circumpolar trough are also related to the errors in the cloud simulations over the tropics, especially over the tropical western Pacific Ocean [*Kiehl et al.*, 1994], where clouds are significantly undersimulated.

The classic semiannual variation in pressure was first described by *Schwerdtfeger and Prohaska* [1956], and more comprehensive studies of this phenomenon can been found in the works of *van Loon* [1967] and *van Loon et al.* [1972]. The semiannual variation mode is affected by the meridional gradient of solar insolation [*Schwerdtfeger*, 1960] and by the interaction between the storms and the Antarctic topography [*Parish et al.*, 1994]. The annual march of the zonally averaged circumpolar trough is exhibited in Figure 2 for the observations and CCM2 simulations. The CCM2 simulated circumpolar trough is closer to the observations in summer than in any other season in terms of intensity and location; the errors of intensity and location are as large as 12 hPa and 3° in winter, respectively. In general, CCM2 oversimulates the intensity of the trough and places it equatorward of the observed location. The semiannual variation of the circumpolar trough is nearly in phase with the observations except during winter. In addition, Figure 2 shows that the differences between the 5-year mean used here and the 20-year mean used by *Hack et al.* [1994] are fairly small. The two observational data sets, ECMWF (1980-1989) and the South African Weather Bureau (1951-1958) and the Australian Bureau of Meteorology (1972-1980) [from *Xu et al.*, 1990], exhibit small differences; the 2° more equatorward location of the former accompanies a 2-hPa increase in intensity. *Hurrel and van Loon* [1994] suggest that the recent 1-month delay in the observed spring decrease in the trough intensity is related to the formation of the Antarctic ozone hole.

In summary, though CCM2 oversimulates the intensity of the trough and places it equatorward of the observed location, the biases are much less than those of CCM1 [*Tzeng et al.*, 1993]. However, the low centers in the sea level pressure field are shifted eastward by about 30° longitude, which is clearly illustrated by the three-wave error pattern in Figure 1c. The semiannual variation of the circumpolar trough is nearly in phase with the observations except during winter.

3.2. Temperature

The surface temperature analysis we use to verify the simulation is from *Giovinetto et al.* [1990], which is probably the most comprehensive and up-to-date estimate available. The surface temperature depiction is based on a compilation of borehole data from 630 sites and of shelter temperatures at 60 meteorological stations. The horizontal distribution of the model's mean annual surface air temperature (Figure 3) is consistent with the observations. The simulated air temperature, however, is about 5°C colder than the observations (Figure 3b) over the entire continent. For example, the simulated minimum temperature over East Antarctica is -68°C, but it is about -62°C in the observations. The observed surface temperature along the coastline is -15°C but is about -20°C in the model. Although the temperature bias is almost uniform over the continent, the causes of this bias are not necessarily the same everywhere.

Figure 4 shows the annual variation of the model's monthly mean surface air temperature at Vostok (in central East Antarctica) and Mawson (on the coast). The simulated surface air temperatures at Vostok are close to the observations in terms of intensity and annual variation, especially in winter (March-October). Moreover, the coreless winter over the plateau is well simulated by

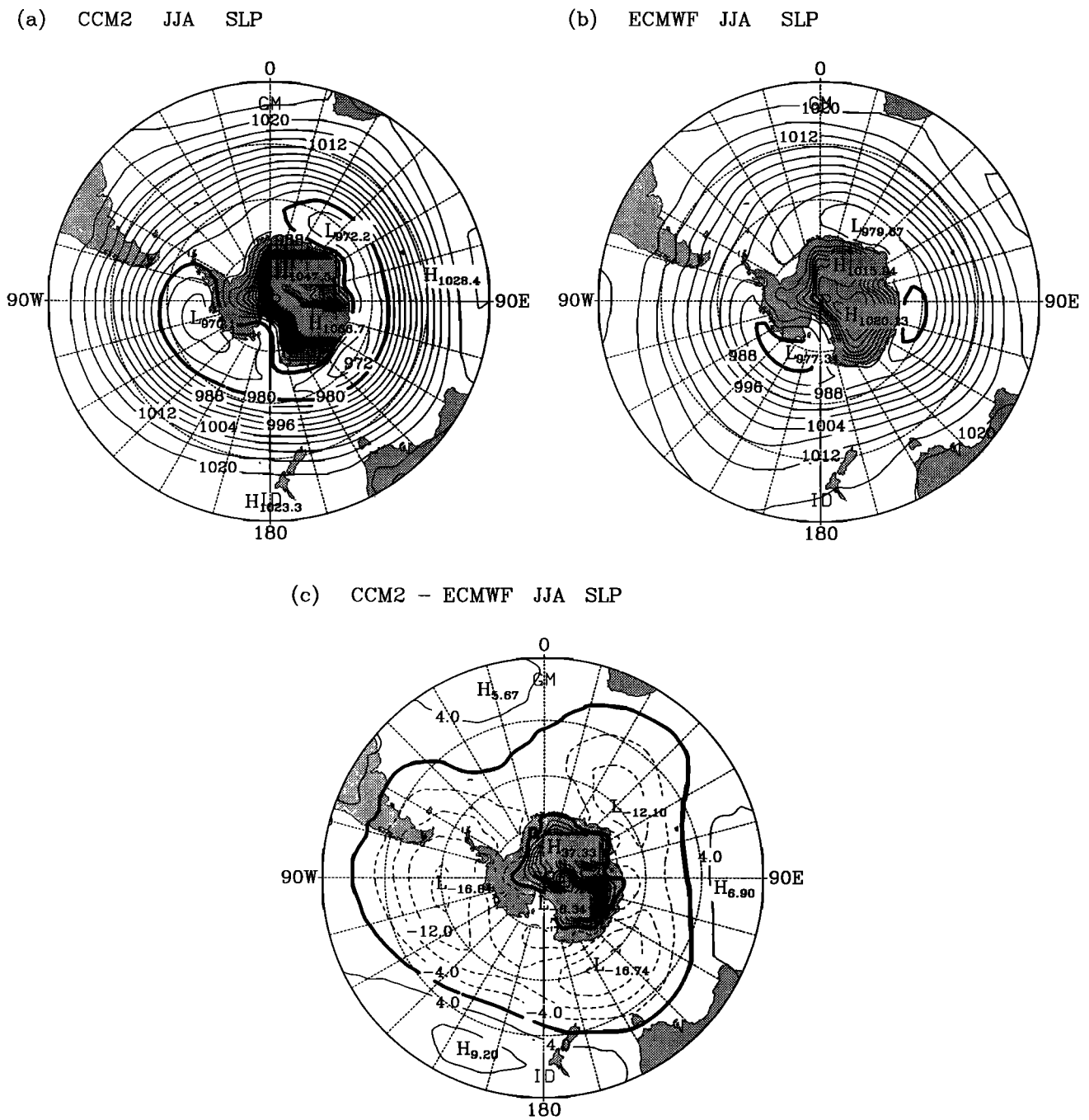

Figure 1. Winter (JJA) mean of sea level pressure (SLP) for (a) climate community model version 2 (CCM2), (b) European Center for Medium-Range Weather Forecasts (ECMWF) analysis, and (c) difference between the CCM2 and ECMWF analysis. Contour interval (CI) is 4 hPa. Contour value of 980 hPa in Figures 1a and 1b is bolded. The zero line in Figure 1c is also bolded. Parallels of latitude are given every 15° starting from 30°S.

the model. The model, however, has a cold bias of about 8°C over the plateau during the nonwinter months (NDJF). A similar result is also found in the French GCM EMERAUDE (with T42 horizontal resolution and 30 vertical levels) using sea surface temperature and sea ice as external forcing [*Pettré and Mahfouf,* 1993]. The cold bias in summer is probably due to the cloud and albedo simulations. The model oversimulates the cloud amount over both polar regions throughout the year. Definitely, the oversimulated cloudiness in nonwinter months prevents a considerable amount of incoming shortwave radiation from reaching the Earth's surface.

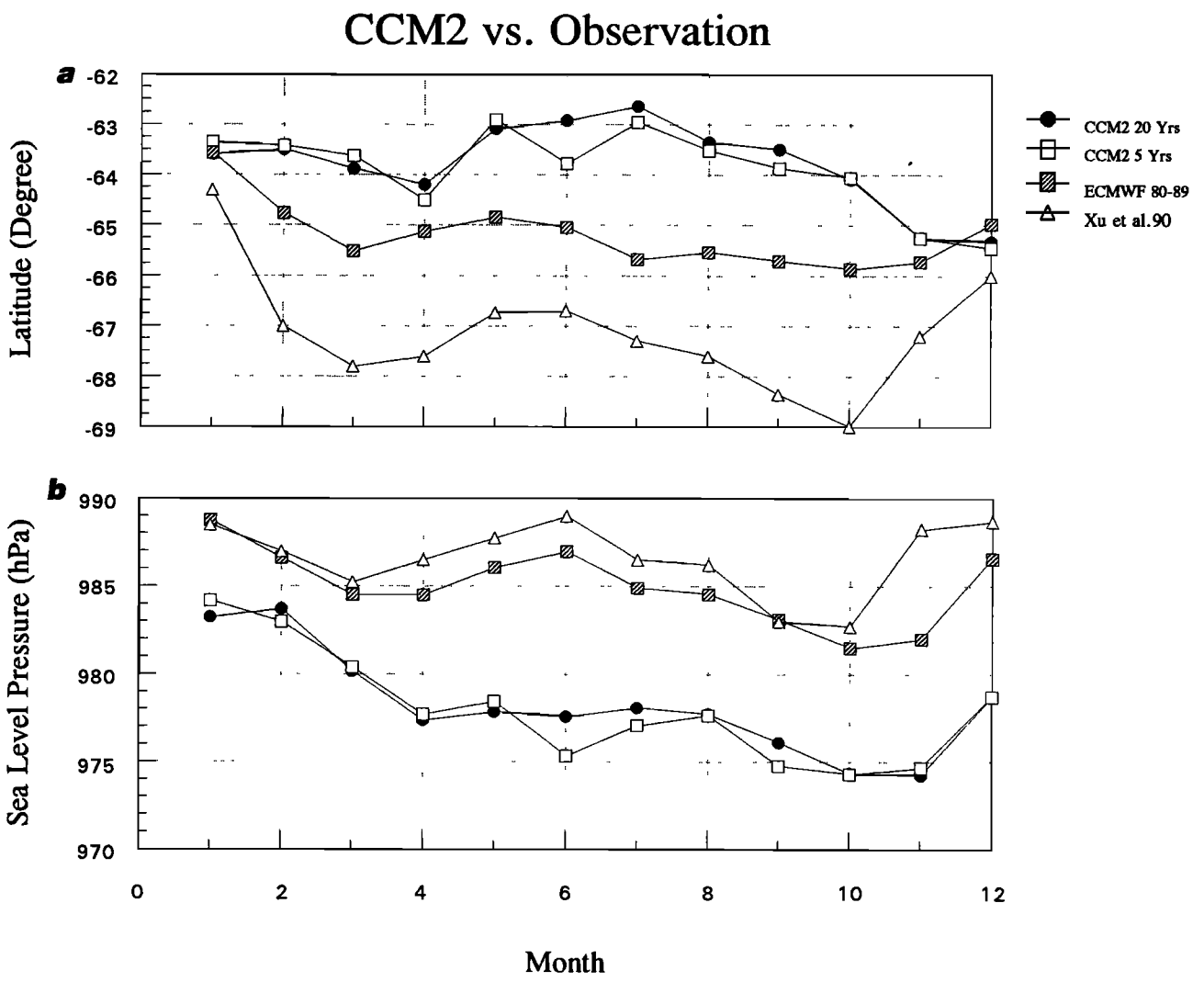

Figure 2. The annual march of the zonally averaged (a) location and (b) intensity of the circumpolar trough for two CCM2 averaging periods and from the observations (ECMWF) [*Xu et al.*, 1990].

Therefore the surface air temperatures are undersimulated. This is also confirmed by the total energy budget analyses in section 3.6.

Over the coastal area the CCM2 suffers a large cold bias (by 10°C) in winter (AMJJAS), which is likely attributable to the uniformly specified 2-m sea-ice thickness and the 100% sea-ice fraction in each sea-ice grid box. *Simmonds and Budd* [1991] pointed out that the mean surface air temperatures over the sea-ice zone increase as the water fraction (leads) increases. A similar conclusion has also been obtained from GCM sensitivity simulations for snow albedo and sea-ice coverage [*Genthon*, 1994]. Moreover, because in reality the thickness of sea ice decreases to zero at the northern edge of the sea-ice zone, the constant thickness of sea ice in the model significantly suppresses the energy flux from the ocean to the atmosphere. Notice also that the temperature series come into agreement near the time of minimum sea-ice extent (JFM).

One of the most prominent characteristics of the Antarctic temperature field is the surface inversion which persists year-around apart from the two summer months. This strong surface inversion is caused by the intense longwave radiative heat loss from the surface under the geographic and atmospheric conditions of Antarctica [*Schwerdtfeger*, 1970]. Figure 5 presents the horizontal distribution of inversion strength from observations [after *Schwerdtfeger*, 1970] and CCM2 for winter (JJA); the latter is calculated as the difference between maximum temperature within the troposphere and surface temperature. The model well captures the intensity and horizontal structure of the inversion over Antarctica. The intensity in CCM2, however, is 5°C stronger than observed over the East Antarctic plateau but about 5°-10°C weaker over the Ross Ice Shelf.

Zonally averaged simulated temperature cross sections for July and January, with the differences from the 1980-1989 ECMWF-analyzed temperature field, are shown in

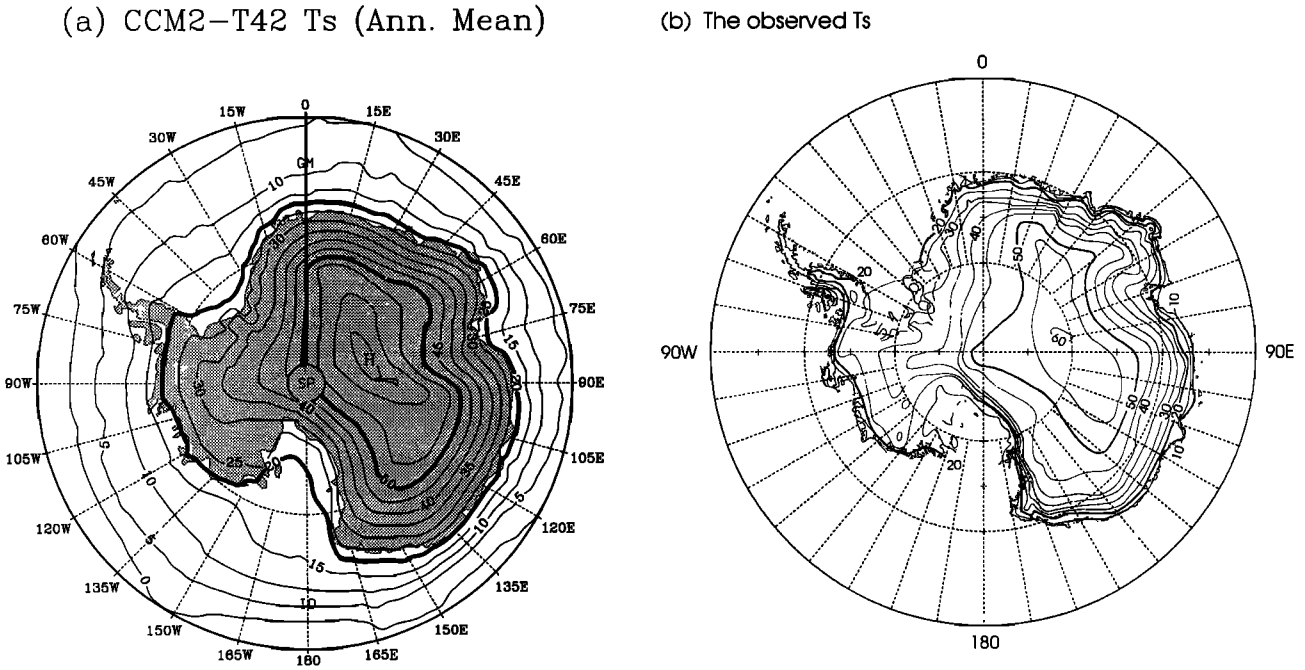

Figure 3. Mean annual surface air temperature (negative °C) for (a) CCM2 and (b) observations [after *Giovinetto et al.,* 1990]. CI is 5°C. The 20°C and 50°C isotherms are bolded. Parallels of latitude start at 60°S.

Figures 6 and 7, respectively. The simulated temperature is generally colder than observed in the entire southern troposphere. Like other Atmospheric General Circulation Models (AGCMs) [*Hack et al.,* 1994], CCM2 continues to have a rather cold middle-and higher-latitude tropopause, which can be from 7.5 K (July) to 16 K (January) colder than the analyses. The warm bias in July over Antarctica near the surface reflects the fact that CCM2 captures the low-level inversion, but the ECMWF analyses do not. Another feature to note in both Figures 6 and 7 is the subtropical midtropospheric warm bias, which has a maximum value of 1.0 K. It is probable that errors in ECMWF-analyzed data over the subtropics before 1989, which are used here, could cause this warm bias [*Trenberth,* 1992; *Hack et al.,* 1994].

3.3. The 500-hPa Height

In winter (JJA) the polar vortex is about 100 gpm too strong in the CCM2. Furthermore, although the model's

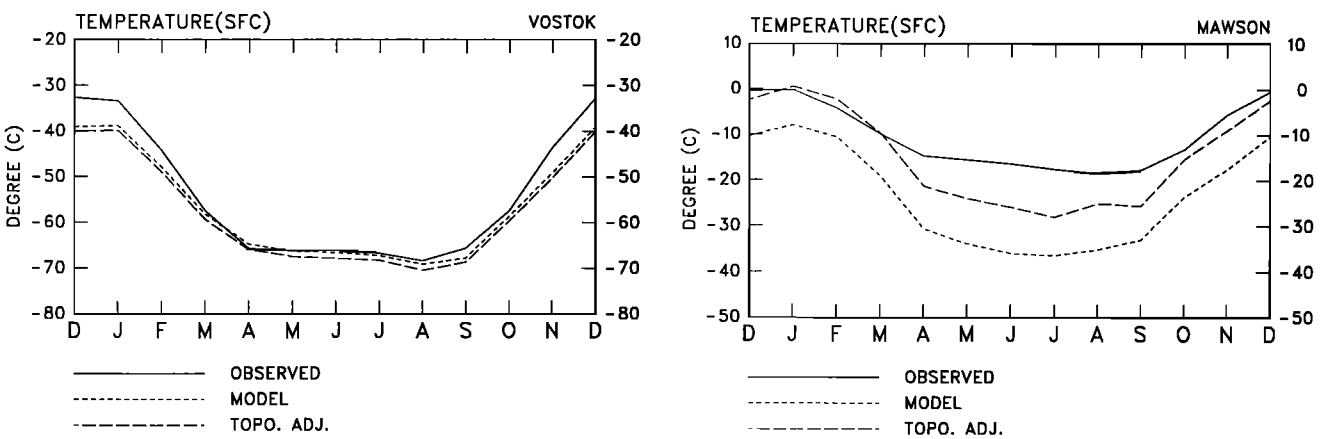

Figure 4. The seasonal cycle of monthly mean surface air temperature (°C) at (a) Vostok (in central East Antarctica) and (b) Mawson (on the coast). The topographic adjustment to the model values accounts for the elevation difference between the nearest model grid point and the station; details are given by *Tzeng et al.* [1993].

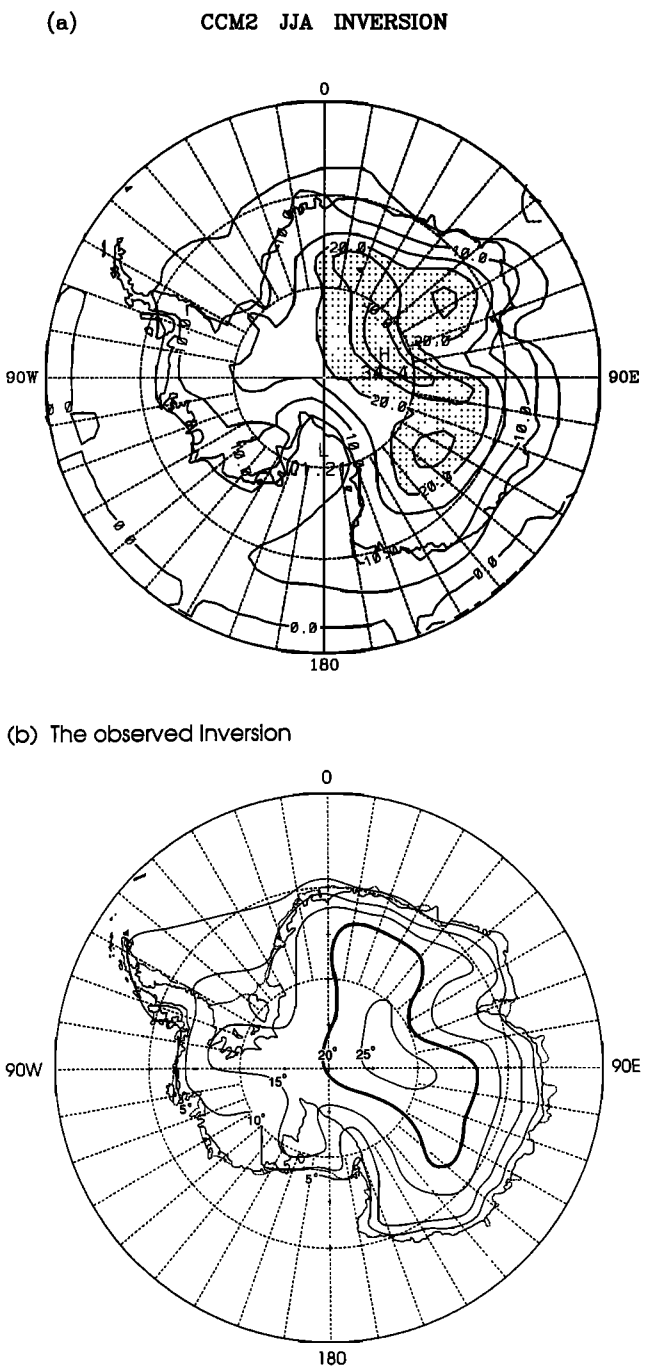

Figure 5. The inversion strength (degrees Celsius) for (a) CCM2 and (b) the observations [after *Schwerdtfeger,* 1970]. CI is 5° C. Values greater than 20° C are stippled in Figure 5a. The 20° C contour is bolded in Figure 5b.

planetary-scale waves have a wavenumber 3 pattern, their axes are shifted eastward by about 15°-60° longitude (Figure 8). The eastward shift of the troughs steers the low centers at sea level and hence the storm tracks. On the other hand, *James*[1988] indicated that Rossby waves can propagate from the tropics to the midlatitudes (about 40° S) and that wavenumber 1 can even reach 75° S. This finding shows that the errors in the simulated clouds and radiation in the tropical and subtropical regions [*Kiehl et al.,* 1994] will directly affect the propagation of Rossby waves through the vortex stretching (divergence) term. Therefore the phase shift of the troughs in the southern hemisphere is also caused by the errors in the cloud optical properties.

The bias in intensity of the polar vortex results from the cold bias of surface temperature, which accelerates the surface winds [*Shibata and Chiba,* 1990] and intensifies the downward motion. Anomalously cold surface temperatures over Antarctica also depress the surface pressure around the continent. Consequently, the circumpolar trough is also related to the oversimulated polar vortex. Because the variation of the intensity of the circumpolar trough is related to tropical heating anomalies [*Meehl,* 1987; *Meehl and Albrecht,* 1988], the errors in the model's cloud properties and simulated radiation budget over the tropics also contribute to the errors in the intensity of the circumpolar trough. The schematic diagram (Figure 9) shows how the errors in the height (and sea level pressure) are inferred to be caused by problems with the low-latitude cloud optical properties.

Because of the intensification of the polar vortex the difference between the CCM2 simulations and ECMWF analyses exhibits a negative anomaly of 500-hPa height and a positive anomaly of SLP over Antarctica. Moreover, the subtropical anticyclones are also oversimulated by the model (not shown). Consequently, the model has a positive anomaly over this region at 500 hPa. The biases of height over Antarctica and the subtropical regions give a positive anomaly of the meridional geopotential height gradient. Therefore the westerlies over the Southern Ocean from 40° to 70° S are also oversimulated by the model.

Figure 10 shows the difference of zonally averaged 500-hPa height between 40° S and 70° S (i.e., the mean zonal geostrophic wind, u_g). The CCM2 zonal geostrophic winds are about 5 m s^{-1} too strong, but their annual and semiannual march are consistent with the observations. The well-reproduced semiannual cycle of the geostrophic wind indicates that the shortcomings of the semiannual cycle in the simulated circumpolar trough are only weakly reflected at 500 hPa.

3.4. Surface and Tropospheric Winds

The CCM2 simulated surface winds at σ = 0.993 (Figure 11), about 50 m above the ice surface, are very consistent with the katabatic wind regime simulated by the mesoscale model of *Parish and Bromwich* [1991], which can produce a realistic katabatic wind regime over the Antarctic continent during winter. Because of the lack

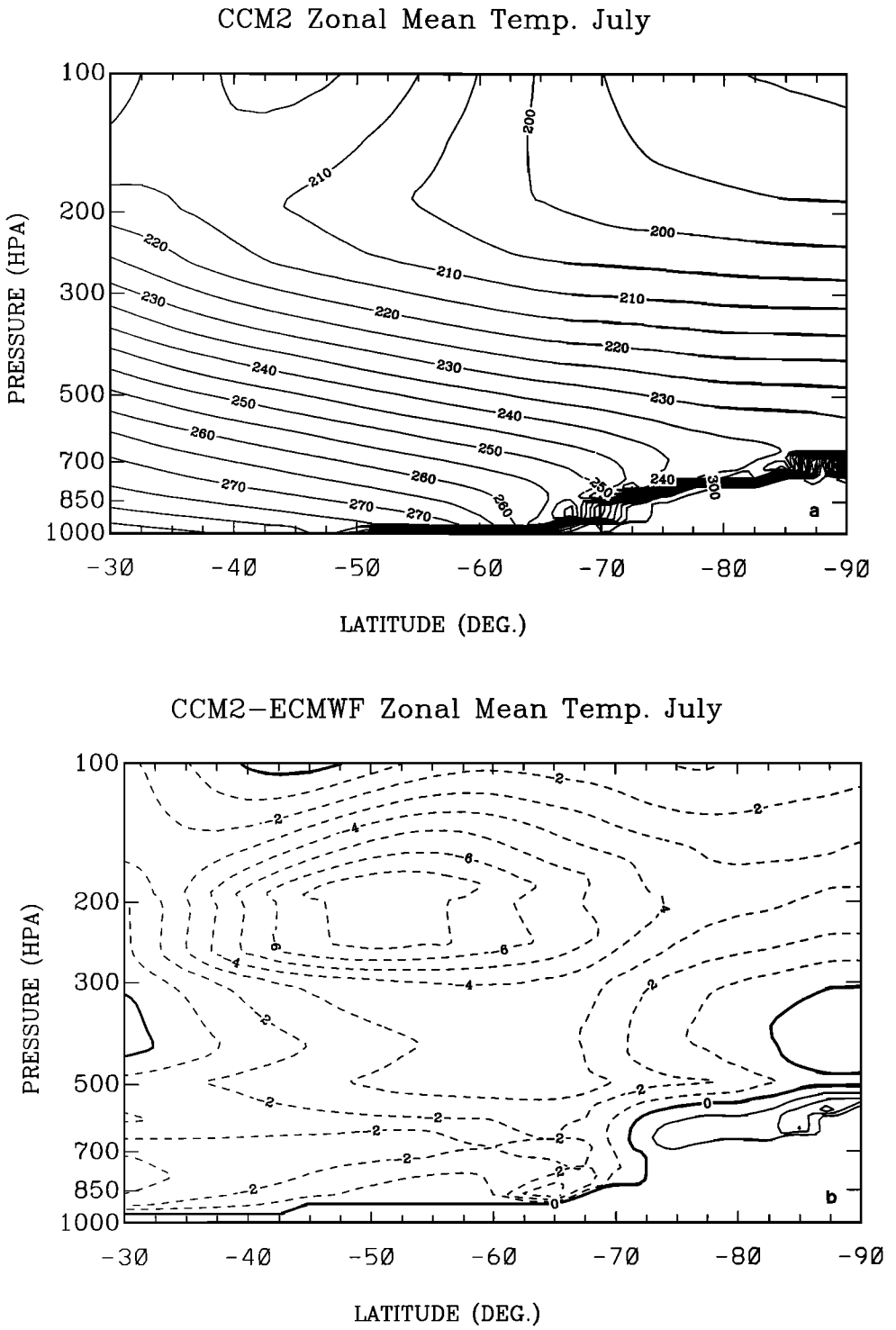

Figure 6. The zonally averaged meridional-vertical cross section of monthly mean temperature for July. (a) CCM2 and (b) difference between CCM2 and the ECMWF analyses. CI is 5 K in Figure 6a and 1 K in Figure 6b.

of comprehensive surface observations during the Antarctic winter, the surface wind simulated by this mesoscale model is used to verify the simulation of CCM2. For example, the simulated maximum wind speed is over the coastal slopes and the minimum wind speed is over the crest of the terrain. Moreover, the convergence zone near the southeastern side of the Ross Ice Shelf (85°S, 150°W) and the low-level jet over MacRobertson Land (60°E) are captured by the model. This achievement clearly results from the comparatively high spatial resolution (and thus

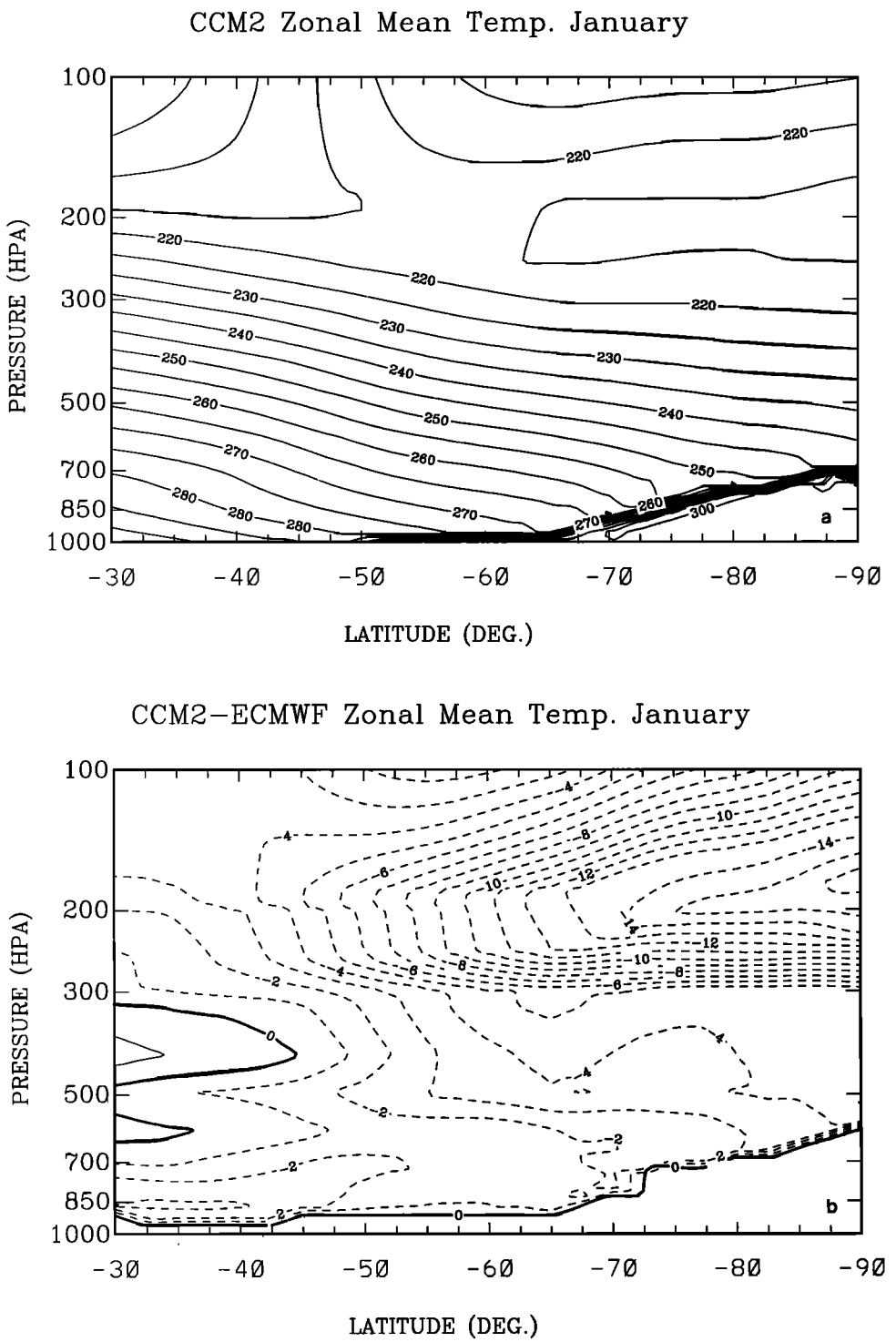

Figure 7. The same as Figure 6 except for January.

reasonable terrain slopes) and the well-captured surface temperature inversion. However, the simulated wind by CCM2 is significantly weaker than that in the mesoscale model. Furthermore, the wind direction in CCM2 is mostly opposite to that simulated by the mesoscale model on the east side of Antarctic Peninsula. This could be caused by both the limited spatial resolution of the CCM2 simulation and the shortcomings in the sensible heat flux parameterization [cf. *Hines et al.*, 1994].

Another notable finding is that the model is able to reproduce the split jet stream in the middle and upper troposphere over the Pacific and Indian oceans during

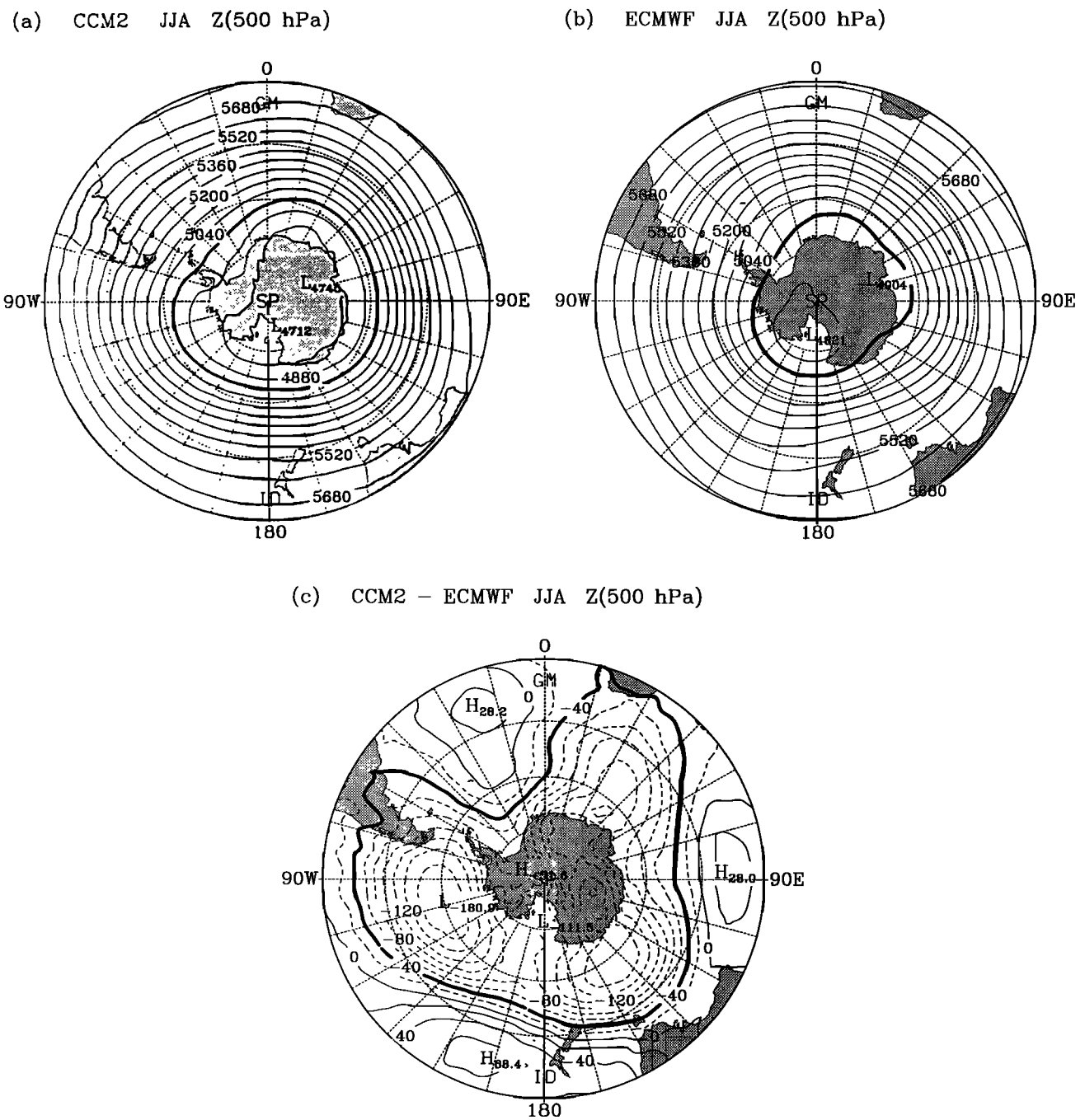

Figure 8. Winter (JJA) mean of height at 500 hPa for (a) CCM2, (b) ECMWF analysis, and (c) difference between the CCM2 and the ECMWF analysis. CI is 80 gpm and 4960 gpm contour line is bolded in Figures 8a and 8b; in Figure 8c, CI is 20 gpm and -40 gpm contour line is bolded. Parallels of latitude are given every 15° starting from 30°S.

winter (Figure 12). This is a big improvement in the model simulation because most AGCMs are not able to capture this feature [*Xu et al.*, 1990]. One should not be surprised by the eastward rotation of the simulated split jet, because the phase of the troughs in the middle and upper troposphere is shifted by the model. Moreover, as discussed in section 3.3, the zonal wind speed in the midlatitudes is oversimulated by the model because of the intensified meridional gradient of geopotential height. However, the strength of the subtropical jet over Australia is slightly underestimated by the model.

3.5. Moisture Budget

The amount of annual snow accumulation simulated over Antarctica and along the coastline by CCM2 is very

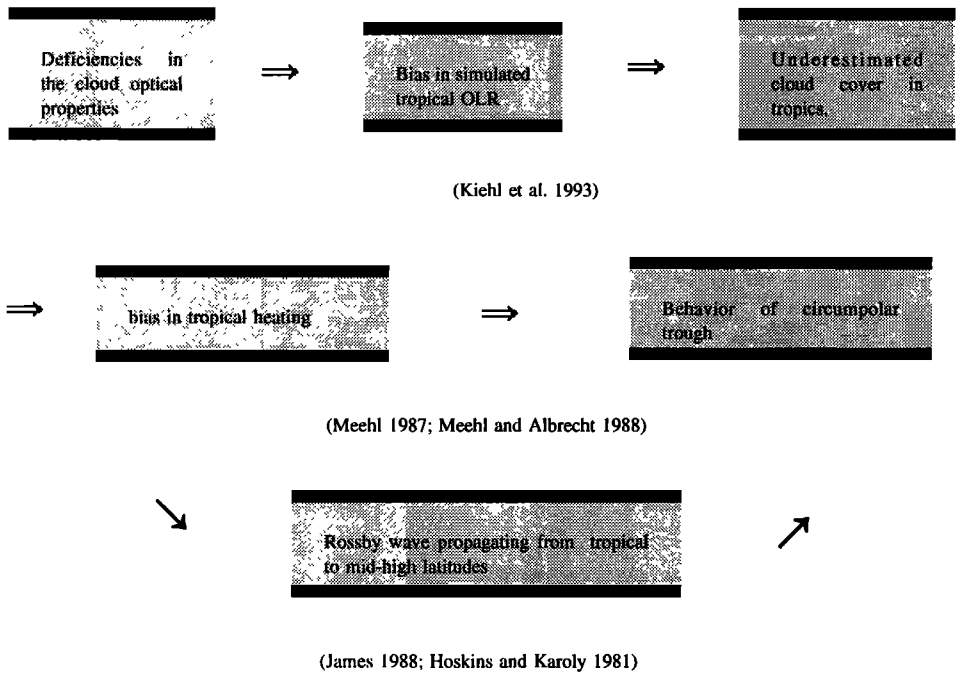

Figure 9. Schematic diagram showing how the polar errors in the height (and sea level pressure) are caused by deficiencies in low-latitude cloud optical properties.

close to the observations (Figure 13). In particular, a very arid climate over the continental interior (less than 5 cm yr^{-1}) is modeled. Also, the accumulation minima (less than 15 cm yr^{-1}) over the Ross Ice shelf and Filchner/ Ronne Ice Shelf are to some extent captured by the model. Although these two accumulation minima are also shown in the CCM1-R15 simulation, the cause of these features in CCM1-R15 is different from that in CCM2-T42. *Tzeng et al.* [1993] indicated that these accumulation minima and the maximum center around the south pole in CCM1-R15 are mainly caused by the spectral truncation error in such a low (R15) resolution model. T42 resolution (42 waves along each latitude circle), however, does not seriously suffer from this type of error.

The moisture budget analysis of the CCM2 (Table 1) shows that the simulated precipitation ([P]) and "evaporation" ([E]) rates are slightly greater than the *Peixoto and Oort* [1992] climatological values; the simulated net precipitation ([P-E]) (15.3 cm/yr) is closer to the latest observational estimate (18.4±3.7 cm/yr) by *Giovinetto et al.* [1992] than the *Peixoto and Oort* [1992] (PO92) result (14.7 cm/yr). The CCM2 moisture transport convergence poleward of 70°S is very close the observed value quoted by *Peixoto and Oort* [1992] but significantly smaller than *Yamazaki*'s [1992] diagnosis which matches *Giovinetto et al.*'s [1992] surface-based [P-E]. The error (residual) of the CCM2 budget equation is quite small (3.3 cm/yr) and approximates that of *Peixoto and Oort* [1992]. This error term is 37.7 cm yr^{-1} in CCM1-R15 over the same region [*Tzeng et al.*, 1993]. The improvement of the moisture budget in CCM2 is attributed to the use of the semi-Lagrangian transport scheme instead of the CCM1 positive moisture fixer scheme. Definitely, the semi-Lagrangian scheme is very good at reproducing the moisture transport into a small area, such as 70°S-SP. The error, however, increases dramatically when the area expands to 60°S-SP and 45°S-SP (Table 1). This error may arise because the semi-Lagrangian scheme is inherently nonconservative, although the scheme itself is shape conserving for each transporting parcel. As the budget domain further increases to 30°S-SP, precipitation is roughly balanced by evaporation and the meridional transport decreases in importance due to the constraint of global water vapor conservation. Thus the error of the budget is reduced as expected.

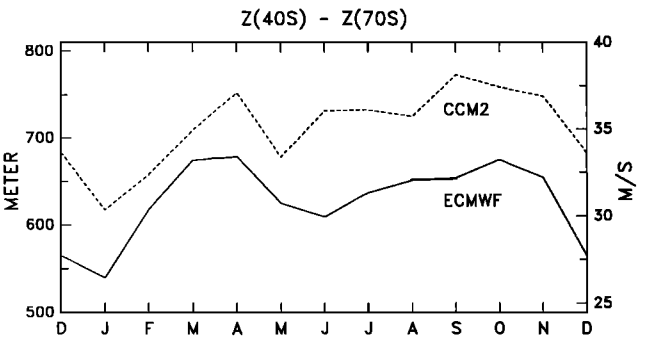

Figure 10. The difference of zonally averaged 500-hPa height between 40°S and 70°S (i.e., the mean zonal geostrophic winds, u_g).

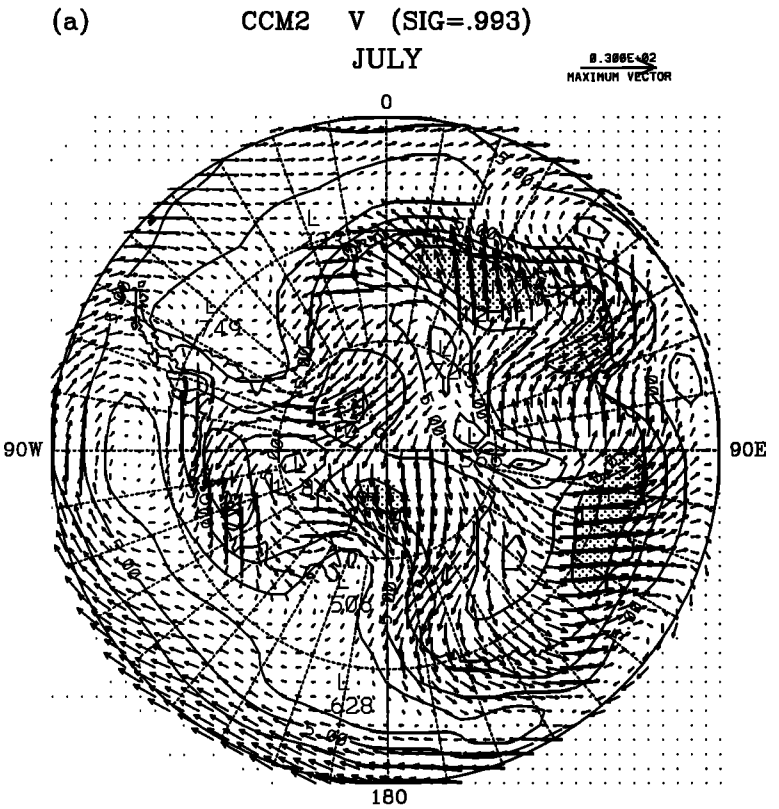

(b) Surface wind for winter – Parish and Bromwich 1991

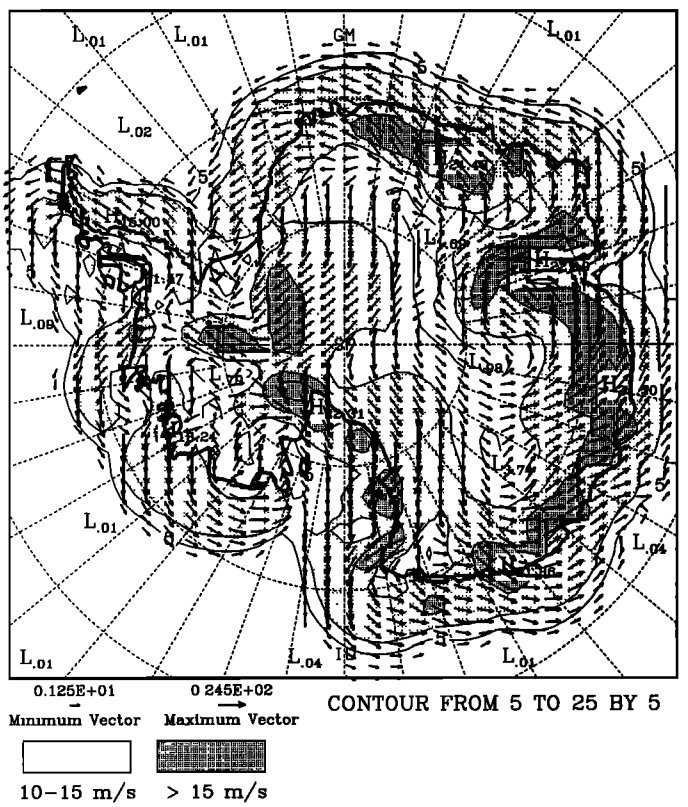

Figure 11. The simulated surface wind vectors and wind speeds by (a) the CCM2 and (b) the mesoscale model of *Parish and Bromwich* [1991]. CI is 2.5 m s^{-1} and values greater than 10 m s^{-1} are stippled in Figure 11a; maximum values of wind speed are less than 15 m s^{-1}. In Figure 11b, CI is 5 m s^{-1}, values between 10 and 15 m s^{-1} are lightly stippled, and values greater than 15 m s^{-1} are heavily stippled.

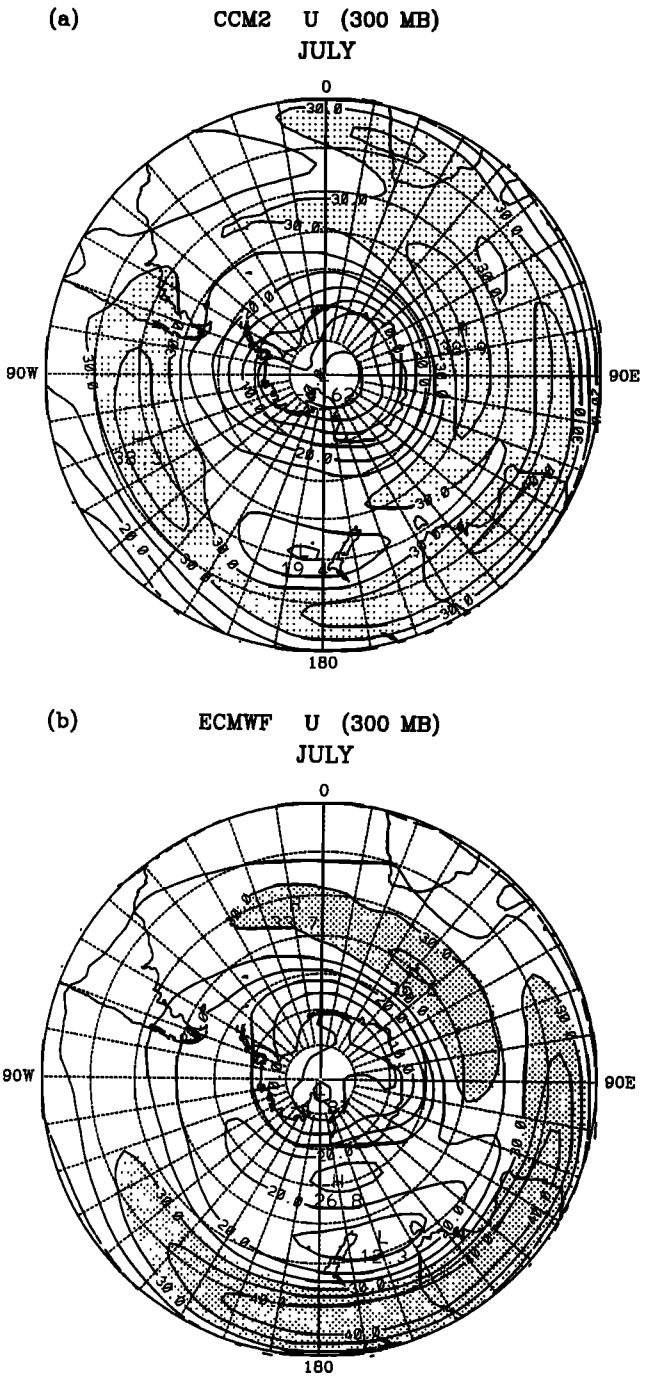

Figure 12. July mean of zonal wind component (u) at 300 hPa for (a) the CCM2 and (b) the ECMWF analyses. CI is 5 m s^{-1}. Values greater than 30 m s^{-1} are stippled.

The annual variations of precipitation, "evaporation" and net precipitation [P-E], for the region poleward of 70° S in CCM2, are displayed in Figure 14 along with the observational estimate of [P-E] by *Yamazaki* [1992], based on National Meteorological Center analyses from 1986 to 1990. The simulated [P-E] rate is a low 0.6 cm/month in early summer and reaches maxima in fall (1.8 cm/month) and late winter (1.6 cm/month), which is in good agreement with the observations. It seems that this weak semiannual oscillation is well represented in CCM2 for area averaged (P-E) over Antarctica in terms of magnitude and phase apart from a variable 1-month phase shift. The annual simulated variation of precipita-

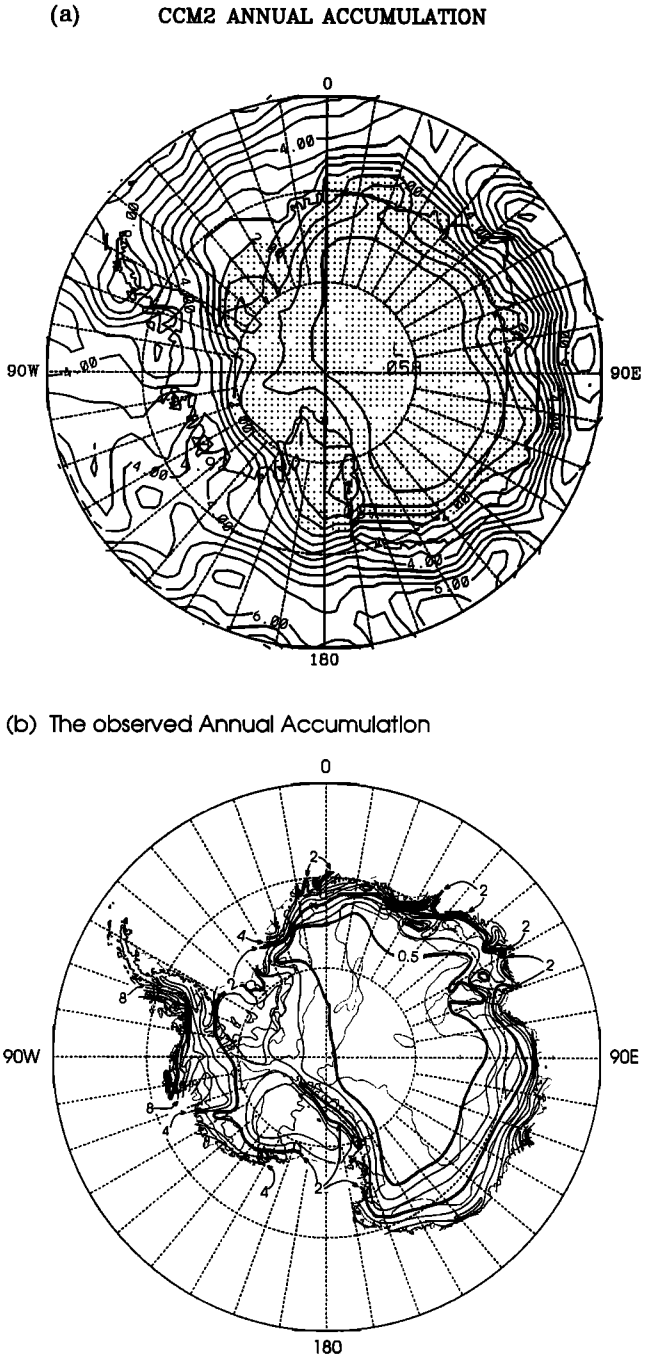

Figure 13. The annual snowfall accumulation (P-E) from (a) CCM2 and (b) the observations [after *Bromwich*, 1988]. Unit is 100 mm yr^{-1}. CI is 0.5 in Figure 13a and variable in Figure 13b. Values less than 2.0 in Figure 13a are stippled. The 0.5 and 2.0 contours in Figure 13b are bolded.

Table 1. Annual Values of the Areally Averaged Precipitation Rate ([P]), Surface Latent Heat Flux ([E]), and the Moisture Transport Convergence Poleward of 70°S ([Q]) From the NCAR CCM2 and Observations

	[P]	[E]	[P-E]	[Q]	Error
GBW92, 70°S-SP			18.4±3.7		
Y92, 70°S-SP				16.2±1.9	
PO92, 70°S-SP	19.0	4.3	14.7	11.6	3.1
CCM2, 70°S-SP	21.6	6.3	15.3	12.0	3.3
CCM2, 60°S-SP	55.7	22.3	33.4	14.2	19.2
CCM2, 45°S-SP	93.2	49.0	44.2	18.0	26.2
CCM2, 30°S-SP	100.8	82.9	17.9	4.6	13.3

Unit is centimeters per year. Moisture budget error is equal to [P-E] - [Q]. GBW92, *Giovinetto et al.* [1992], climatological average from surface observations. Y92, *Yamazaki* [1992], climatological average from National Meteorological Center analyses for 1986-1990. PO92, *Peixoto and Oort* [1992], climatological average. NCAR, National Center for Atmospheric Research; CCM2, community climate model version 2.

tion over Antarctica reaches a primary maximum in fall with two other peaks in August and December and minima in July, September, and January. The observed annual cycle of areally averaged precipitation poleward of 70°S is not well known, although most of East Antarctica has a winter maximum and summer minimum, whereas the semiannual variation is expressed somewhat in West Antarctica and becomes dominant on the west side of the Antarctic Peninsula [*Bromwich*, 1988; *Dolgina and Petrova*, 1977]. It appears that the modeled precipitation should exhibit a more well-defined summer minimum. By contrast, the surface latent heat flux (would be mostly sublimation over Antarctica) exhibits a smooth variation with a peak during summer and minimum values during winter. Observed ice sheet values are larger than previously thought [*Budd and Simmonds*, 1991; *Stearns and Weidner*, 1993] and an annual cycle like that simulated has been measured at one point [*Fujii and Kusunoki*, 1982]. If the modeled [P] and [E] rates are approximately correct, then because the poleward moisture transport convergence is small during summer, most of the moisture evaporated or sublimated from the surface during summer must be precipitated out poleward of 70°S.

3.6. Total Energy Budget

Kiehl et al. [1994] found that the clouds in CCM2 reflect an insufficient amount of solar radiation in the middle latitudes, especially during summer. By contrast, the simulated net incoming shortwave radiation at top of the atmosphere over the south polar cap (70°S to south pole) during summer is still smaller than the observations (Table 2). This is because the model's cloudiness and planetary albedo are too large over this region and hence block a large amount of the incoming shortwave radiation. These biases result in anomalously cold surface temperatures over the plateau in summer. Figure 15 shows the winter zonally averaged cross section of

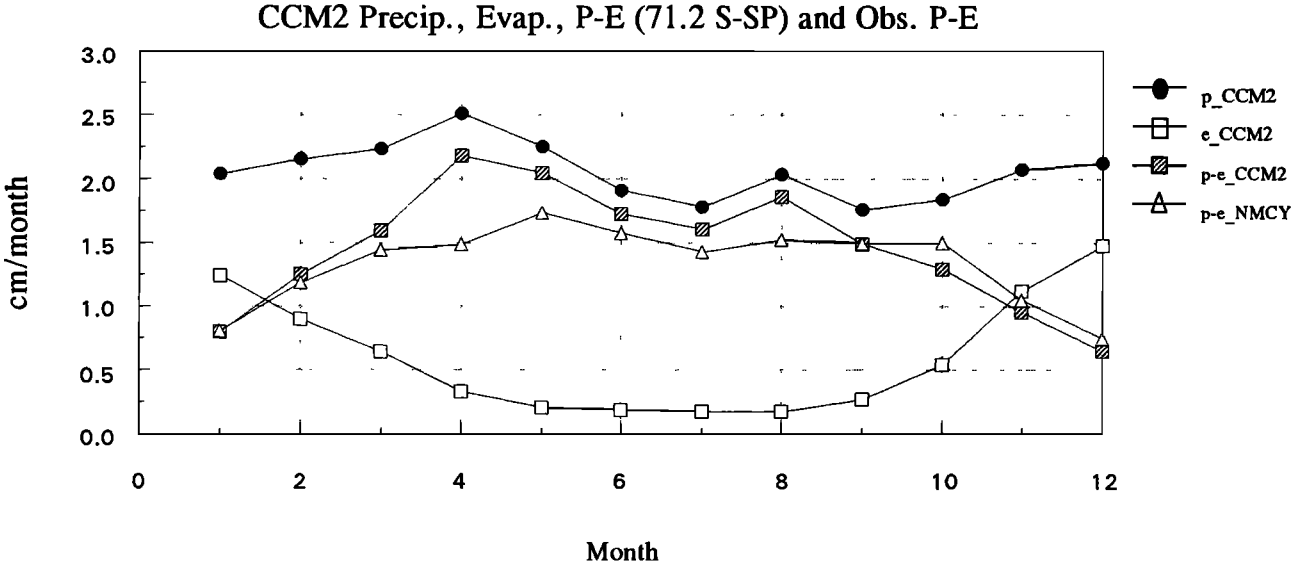

Figure 14. The annual variations of precipitation, surface latent heat flux, and (P-E) from the CCM2 and the observations (Q) [from *Yamazaki*, 1992]. Unit is centimeters per month.

Table 2. Winter (JJA) and Summer (DJF) Means of Various Energy Componentsof the South Polar Cap

	F_{sw}	F_{lw}	F_{top}	TF	SF	F_{adv}	F_{sfc}	Res
				Winter Mean (JJA)				
CCM2	0.9	-137.7	-136.8	59.3	35.6	94.9	12.0	-29.0
NO88*	0.7	-128.7	-128.0	32.7	104.?	136.7+	6.7	15.4
				Summer Mean (DJF)				
CCM2	148.5	-185.5	-37.0	22.5	4.4	26.9	-8.4	-18.5
NO88	160.0	-192.0	-32.0	15.0	27.3?	42.3+	-29.3	-19.0

Units are in watts per square meter. F_{sw}, shortwave radiation into the top of atmosphere; F_{lw}, longwave radiation into the top of atmosphere; F_{top}, net energy flux into the top of atmosphere; TF, transient energy flux across 70°S; SF, standing energy flux across 70°S (which includes SE, MMC, and NMF of NO88); F_{adv}, total energy flux across 70°S; F_{sfc}, net energy flux into the atmosphere from the Earth's surface; Res, residual of the energy budget equation ($Res=F_{top}+F_{adv}+F_{sfc}$).

* NO88, data from *Nakamura and Oort* [1988].

\+ Evaluated from a general circulation model by NO88 (not observations).

meridional circulation and cloudiness in the CCM2. Although the polar direct cell (sinking poleward of 70°S and rising motion equatorward of 70°S) is qualitatively well simulated by CCM2, the associated cloud fraction indicates that the Antarctic is almost overcast by thick cloud from near surface to tropopause. The cloud coverage from CCM2 is very similar to CCM1 [*Tzeng et al.*, 1993]. Though there are many difficulties estimating cloud cover in the polar regions [*Rossow*, 1992], the coverage determined from surface observations [*Schwerdtfeger*, 1970; *van Loon et al.*, 1972] and high-resolution satellite Advanced Very High Resolution Radiometer imagery [*Yamanouchi and Kawaguchi*, 1992] is less than four tenths over the Antarctic continent. In fact, the simulated cloud coverage in CCM2 has a maximum over Antarctica where the cloud cover is even larger than that near the oceanic storm track. This is opposite to the observations. The reasons for this cloudiness error are probably the spectral truncation and computational roundoff because a spectral model is very sensitive to these two factors over high latitudes. Moreover, both the north and the south polar regions suffer from this bias. The remedy for the oversimulated cloud amount in the Antarctic cannot be simply "to turn these extra clouds off." In nature there are numerous feedbacks among atmospheric radiation, dynamics, and cloud microphys-

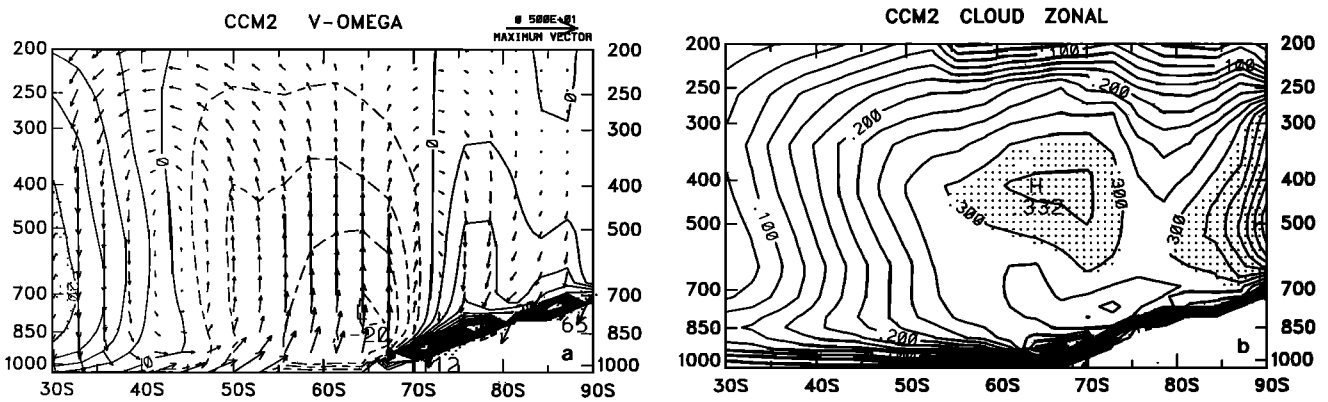

Figure 15. The monthly (July), zonal average of CCM2 simulated (a) meridional-vertical wind vectors (v omega) along with zonal mean omega values (contours) and (b) cloudiness (fraction). CI in Figure 15a is $5x10^{-4}$ hPa s^{-1} and values greater than $20x10^{-4}$ hPa s^{-1} are stippled. Values greater than 0.3 are stippled in Figure 15b.

ics. *Shibata and Chiba* [1990] found that the Japan Meteorological Research Institute (MRI) global spectral model simulation of Antarctic near-surface temperature, winds, and circumpolar trough was sensitive to the specified emissivity of clouds over the Antarctic continent. To understand how the various parameterizations of radiative, dynamical, and microphysical processes in CCM2 might be generating the anomalous cloud cover, a first step in this direction might be to observe how the model responds to changes in cloud radiative properties (e.g., emissivity of cloud) over Antarctica (D. Lubin, personal communication, 1994).

Over the south polar cap, the model emits more longwave radiation to outer space (Table 2) than the observations in winter (JJA) but less in summer (DJF). The result in summer over this region is different from most of the remainder of the Earth where the model emits too much radiation to space [*Kiehl et al.*, 1994]. This difference results from the anomalously high cloudiness, particularly in the middle and upper troposphere. Although there are errors in both longwave and shortwave radiation, the net energy budget at the top of the atmosphere is close to that observed. The more serious shortcoming in the energy budget is found in the advection of energy ($C_pT+gz+Lq$) flux across 70°S. Table 2 shows that the standing energy flux (SF), which is defined as the stationary part of the advection of the energy [*Nakamura and Oort*, 1988], has the greatest bias in both winter and summer seasons. This bias may result from the errors in the simulated planetary-scale waves, which is attributed to the errors in the cloud simulation over the tropics and midlatitudes. The transient flux (TF) is overestimated during both winter and summer, most likely as a result of the oversimulated circumpolar trough, but does not compensate for the major SF underestimates.

4. Conclusion

The CCM2 simulation of the circumpolar trough (sea level pressure), surface air temperatures, the polar vortex, surface and upper level winds, vertical motion, cloudiness, precipitation, and moisture and energy budgets are analyzed to validate the performance of the model. The results show that the model well simulates most of the important climatological features over the high southern latitudes, such as the circumpolar trough, the coreless winter over the plateau, the intensity and horizontal distribution of the surface inversion, the speed and streamline pattern of the katabatic winds, the double jet stream feature over the southern Indian and Pacific oceans, and the arid climate over the continent.

These improvements are due to (1) the higher horizontal resolution, (2) the semi-Lagrangian scheme for transporting moisture, and (3) the new parameterizations for cloud and radiation. By contrast, the incorporation of these new physical parameterizations does not necessarily result in a better climate simulation. *Kiehl et al.* [1994] found that the model's clouds do not reflect enough shortwave radiation and allow too much longwave radiation to be emitted to space. These errors result in anomalously warm surface temperatures over the tropics and midlatitudes (particularly in the northern summer (JJA)) and hence too much heating over these regions. This excessive heating, in turn, affects the simulated planetary-scale waves globally. Moreover, the oversimulated circumpolar trough during winter, which results in the simulated semiannual variation of the circumpolar trough having the opposite phase to the observations, is due to the errors in the simulated radiation (Figure 9). By contrast, the cold biases over the interior and coastal areas may be due to different factors. The model simulates too much cloud over the continent in summer and hence blocks a considerable amount of incoming solar radiation. However, the cold bias near the coastal regions is attributed to the constant specified thickness of sea ice (2 m). This greatly reduces the energy flux from the ocean to the atmosphere, compared to that which actually occurs through leads and thinner sea ice over most parts of the sea-ice region.

Finally, as a consequence of these generally good results, CCM2 can be used to study broadscale (but not regional) climate change over high southern latitudes. This represents a substantial improvement in performance in comparison to the earlier CCM1 [*Tzeng et al.*, 1993].

Acknowledgments. This paper was supported in part by NASA grants NAGW-2718 (DHB) and NAGW-2666 (TRP) and in part by an internal grant of The Ohio State University (RYT). The computations were mostly performed on the CRAY Y-MP of NCAR and in part on the CRAY Y-MP of the Ohio Supercomputer Center, which is supported by the State of Ohio. The CPU time on the NCAR CRAY Y-MP was provided by CRAY Research Inc. We wish to recognize Beth Daye and John Nagy for their work on the graphics, contribution 915 of Byrd Polar Research Center, The Ohio State University.

References

Alexander, R. C., and R. L. Mobley, Monthly averaged sea-surface temperatures and ice-pack limits on 1° global grid, *Mon. Weather Rev., 104*, 143-148, 1976.

Boville, B. A., Sensitivity of simulated climate to model resolution, *J. Clim., 4*, 469-485, 1991.

Bromwich, D.H., Snowfall in high southern latitudes, *Rev. Geophys., 26*(1), 149-168, 1988.

Bromwich, D.H., J.F. Carrasco, Z. Liu, and R.-Y. Tzeng, Hemispheric atmospheric variations and oceanographic impacts associated with katabatic surges across the Ross Ice Shelf, Antarctica, *J. Geophys. Res., 98*, 13,045-13,062, 1993.

Bromwich, D.H., R.-Y. Tzeng, and T.R. Parish, Simulation of the modern Arctic climate by the NCAR CCM1, *J. Clim., 7*, 1051-1069, 1994.

Budd, W. F., and I. Simmonds, The impact of global warming on the Antarctic mass balance and global sea level, in *International Conference on the Role of the Polar Regions in Global Change*, vol. II, pp. 489-494, University of Alaska, Fairbanks, 1991.

Dolgina, I. M., and L. S. Petrova (Eds.), *Handbook of Antarctic Climate* (in Russian), vol. 2, Gidrometeoizdat, Leningrad, 1977.

Egger, J., Topographic wave modification and the angular momentum balance of the Antarctic troposphere, *J. Atmos. Sci., 49*, 327-334, 1992.

Fujii, Y., and K. Kusunoki, The role of sublimation and condensation in the formation of ice sheet surface at Mizuho Station, Antarctica, *J. Geophys. Res., 87*, 4293-4300, 1982.

Genthon, C., Antarctic climate modeling with general circulation models of the atmosphere, *J. Geophys. Res., 99*, 12,953-12,961, 1994.

Giovinetto, M.B., N.M. Waters, and C.R. Bentley, Dependence of Antarctic surface mass balance on temperature, elevation, and distance to open ocean, *J. Geophys. Res., 95*, 3517-3531, 1990.

Giovinetto, M.B., D.H. Bromwich, and G. Wendler, Atmospheric net transport of water vapor and latent heat across 70°S, *J. Geophys. Res., 97*, 917-930, 1992.

Hack, J.J., Parameterization of moist convection in the NCAR community climate model (CCM2), *J. Geophys. Res., 99*, 5551-5568, 1994.

Hack, J.J., B.A. Boville, B.P. Briegleb, J.T. Kiehl, P.J. Rasch, and D.L. Williamson, Description of the NCAR community climate model (CCM2), *NCAR Tech. Note, NCAR/TN-382+STR*, 108 pp., Natl. Cent. for Atmos. Res., Boulder, Colo., 1993.

Hack, J.J., B.A. Boville, J.T. Kiehl, P.J. Rasch, and D.L. Williamson, Climate statistics from the NCAR community climate model (CCM2), *J. Geophys. Res.*, in press, 1994.

Hansen, J., G. Russell, D. Rind, P. Stone, A. Lacis, S. Lebedeff, R. Ruedy, and L. Travis, Efficient three-dimensional global models for climate studies: Model I and II, *Mon. Weather Rev., 111*, 609-662, 1983.

Hart, T. L., W. Bourke, B. J. McAvaney, and B. W. Forgan, Atmospheric general circulation simulations with the BMRC global spectral model: The impact of revised physical parameterizations, *J. Clim., 3*, 436-459, 1990.

Herman, G.F., and R. Goody, Formation and persistence of summertime Arctic stratus clouds, *J. Atmos. Sci., 33*, 1537-1553, 1976.

Hines, K. M., D. H. Bromwich, and T. R. Parish, A mesoscale modeling study of the atmospheric circulation of high southern latitudes. *Mon. Weather Rev.*, in press, 1994.

Hoskins, B. J., and D. J. Karoly, The steady linear response of a spherical atmosphere to thermal and orographic forcing. *J. Atmos. Sci., 38*, 1179-1196, 1981.

Hurrel, J. W., and H. van Loon, A modulation of the atmospheric annual cycle in the Southern Hemisphere, *Tellus, 46A*, 325-338, 1994.

Hurrel, J. W., J. J. Hack, and D. P. Baumhefner, Comparison of NCAR community climate model (CCM) climates, *NCAR Tech. Note, NCAR/TN-395+STR*, 335 pp., Natl. Cent. for Atmos. Res., Boulder, Colo., 1993.

Intergovernmental Panel on Climate Change (IPCC), *Climate Change*, edited by J. T. Houghton, G.J. Jenkins, and J.J. Ephraums, 365 pp., Cambridge University Press, Cambridge, New York, 1990.

James, I.N., On the forcing of planetary-scale Rossby waves by Antarctica, *Q. J. R. Meteorol. Soc., 114*, 619-637, 1988.

Kiehl, J.T., J.J. Hack, and B.P. Briegleb, The simulated earth radiation budget of the NCAR CCM2 and comparisons with the Earth Radiation Budget Experiment (ERBE), *J. Geophys. Res.*, in press, 1994.

Manabe, S., J. Smagorinsky, and R. F. Stricker, Simulated climatology of a general circulation model with a hydrologic cycle, *Mon. Weather Rev., 93*, 769-798, 1965.

Meehl, G.A., The annual cycle and interannual variability in the tropical Pacific and Indian Ocean regions, *Mon. Weather Rev., 115*, 27-50, 1987.

Meehl, G.A., and B. A. Albrecht, Tropospheric temperatures and the Southern Hemisphere circulation, *Mon. Weather Rev., 116*, 953-960, 1988.

Nakamura, N., and A.H. Oort, Atmospheric heat budgets of the polar regions, *J. Geophys. Res., 93*, 9510-9524, 1988.

Parish, T.R., and D.H. Bromwich, Continental-scale simulation of the Antarctic katabatic wind regime, *J. Clim., 4*, 136-146, 1991.

Parish, T.R., D.H. Bromwich, and R.-Y. Tzeng, On the role of the Antarctic continent in forcing large-scale circulations in the high southern latitudes, *J. Atmos. Sci.*, in press, 1994.

Peixoto, J.P., and A.H. Oort, *Physics of Climate*, 520 pp., American Institute of Physics, New York, 1992.

Pettré, P., and J.F. Mahfouf, Comparison of GCM simulations with some aspects of the climatology of Adelie Land, East Antarctica, preprint volume, in *Fourth International Conference on Southern Hemisphere Meteorology and Oceanography*, pp. 455-456, American Meteorological Society, Boston, Mass., 1993.

Ramanathan, V., E. J. Pitcher, R. C. Malone, and M. L. Blackmon, The response of a spectral general circulation model to refinements in radiative processes, *J. Atmos. Sci., 40,* 605-630, 1983.

Randall, D.A., J.A. Abeles, and T.G. Corsetti, Seasonal simulations of the planetary boundary layer and boundary-layer stratocumulus clouds with a general circulation model, *J. Atmos. Sci., 42,* 641-676, 1985.

Rasch, P.J., and D.L. Williamson, Computational aspects of moisture transport in global models of the atmosphere, *Q. J. R. Meteorol. Society, 116,* 1071-1090, 1990.

Rossow W. B., Polar cloudiness: Some results from ISCCP and other cloud climatologies, in *Third Conference on Polar Meteorology and Oceanography,* pp. 1-3, American Meteorological Society, Boston, Mass., 1992.

Schwerdtfeger, W., The seasonal variation of the strength of the southern circumpolar vortex, *Mon. Weather Rev., 88,* 203-208, 1960.

Schwerdtfeger, W., The climate of the Antarctic, *World Surv. Climatol., 14,* 253-355, 1970.

Schwerdtfeger, W., and F. Prohaska, The semi-annual pressure oscillation, its cause and effects, *J. Meteorol.,* 13, 217-218, 1956.

Shea, D. J., K. E. Trenberth, and R. W. Reynolds, A Global Monthly Sea Surface Temperature Climatology, *NCAR Tech. Note, NCAR/TN-345+STR,* 167 pp., Natl. Cent. for Atmos. Res., Boulder, Colo., 1990.

Shibata, K., and M. Chiba, Effects of radiation scheme on the surface temperature and wind over the Antarctic and on circumpolar lows, *Proc. NIPR Symp. Polar Meteorol. Glaciol., 3,* 36-45, 1990.

Simmonds, I., and W.F. Budd, Sensitivity of the southern hemisphere circulation to leads in the Antarctic pack ice, *Q. J. Meteorol. Soc., 117,* 1003-1024, 1991.

Slingo, J. M., The development and verification of a cloud prediction scheme for the ECMWF model, *Q. J. R. Meteorol. Soc., 113,* 899-927, 1987.

Stearns, C. R., and G. A. Weidner, Sensible and latent heat flux estimates in Antarctica, in *Antarctic Meteorology and Climatology: Studies Based on Automatic Weather Stations, Antarct. Res. Ser., vol. 61,* edited by D. H. Bromwich and C. R. Stearns, pp. 109-138, AGU, Washington, D.C., 1993.

Trenberth, K. E., Global analyses from ECMWF and atlas of 1000 to 10 mb circulation statistics, *NCAR Tech. Note, NCAR/TN-373+STR,* Natl. Cent. for Atmos. Res., 191 pp., Boulder, Colo., 1992.

Tzeng, R.-Y., D.H. Bromwich, and T.R. Parish, Present-day Antarctic climatology of the NCAR Community Climate Model Version 1, *J. Clim., 6,* 205-226, 1993.

van Loon, H., The half-yearly oscillations in middle and high southern latitudes and the coreless winter, *J. Atmos. Sci., 56,* 497-515, 1967.

van Loon, H., J.J. Taljaard, T. Sasamori, J. London, D.V. Hoyt, K. Labitzke, and C.W. Newton, in *Meteorology of the Southern Hemisphere, Meteorol. Monogr. Ser.,* vol. 13, edited by C. W. Newton, 263 pp., American Meteorological Society, Boston, Mass., 1972.

Williamson, D.L., and P.J. Rasch, Water vapor transport in the NCAR CCM2, *Tellus, 46*(A), 34- 51, 1994.

Xu, J.-S., H. Von Storch, and H. van Loon, The performance of four spectral GCMs in the Southern Hemisphere: The January and July climatology and the semiannual wave, *J. Clim., 3,* 53-70, 1990.

Yamanouchi, T., and S. Kawaguchi, Cloud distribution in the Antarctic from AVHRR data and radiation measurements at the surface, *Int. J. Remote Sens., 13,* 111-127, 1992.

Yamazaki, K., Moisture budget in the Antarctic atmosphere, *Proc. NIPR Symp. Polar Meteorol. Glaciol., 6,* 36-45, 1992.

D.H. Bromwich and B. Chen, Polar Meteorology Group, Byrd Polar Research Center, Ohio State University, 108 Scott Hall, 1090 Carmack Road, Columbus, OH 43210-1002.

T.R. Parish, Department of Atmospheric Science, University of Wyoming, Laramie, WY 82071.

R.-Y. Tzeng, Department of Atmospheric Sciences, National Central University, Chungli, Taiwan 320, Republic of China.

(Received March 30, 1994; revised August 15, 1994; accepted August 17, 1994.)